

Article

Bioactive Components of *Myracrodruon urundeuva* against SARS-CoV-2: A Computational Study

Sabrina Kelly Silva Alves ¹, Cássio Silva Sousa ¹ , Edilanne Katrine Amparo Viana ¹, Hellen Cris Araújo Souza ¹, Maycon Douglas Araújo Souza ¹, Arthur Serejo Neves Ribeiro ¹, Vanessa de Sousa do Vale ¹, Muhammad Torequl Islam ², Joabe Lima Araújo ^{3,*}  and Jefferson Almeida Rocha ¹

¹ Research Group on Medicinal Chemistry and Biotechnology, Federal University of Maranhão, São Bernardo 65550-000, Brazil; ja.rocha@ufma.br (J.A.R.)

² Department of Pharmacy, Bangabandhu Sheikh Mujibur Rahman Science and Technology University, Gopalganj 8100, Bangladesh

³ Department of Genetics and Morphology, Darcy Ribeiro University Campus, Brasília 70910-900, Brazil

* Correspondence: joabearaujobiotec@gmail.com

Abstract: SARS-CoV-2 (severe acute respiratory distress syndrome coronavirus 2) is the causative agent for the novel coronavirus disease 2019 (COVID-19). It raises serious biosecurity questions due to its high contagious potential, thereby triggering rapid and efficient responses by the scientific community to take necessary actions against viral infections. Cumulative scientific evidence suggests that natural products remain one of the main sources for pharmaceutical consumption. It is due to their wide chemical diversity that they are able to fight against almost all kinds of diseases and disorders in humans and other animals. Knowing the overall facts, this study was carried out to investigate the chemical interactions between the active constituents of a promising medicinal plant, *Myracrodruon urundeuva*, and some specific proteins of SARS-CoV-2. For this, we used molecular docking to predict the most appropriate orientation by binding a molecule (a ligand) to its receptor (a protein). The best results were evaluated by screening their pharmacokinetic properties using the online tool pkCSM. Findings suggest that among 44 chemical compounds of *M. urundeuva*, agathisflavone, which is abundantly present in its leaf, exhibited excellent molecular affinity (-9.3 to -9.7 kcal.mol⁻¹) with three functional proteins, namely, Spike, M^{Pro}, and RBD of SARS-CoV-2. In conclusion, *M. urundeuva* might be a good source of antiviral agents. Further studies are required to elucidate the exact mechanism of action of the bioactive compounds of *M. urundeuva* acting against SARS-CoV-2.

Keywords: *Myracrodruon urundeuva*; molecular docking; SARS-CoV-2; pharmacokinetic properties



Citation: Alves, S.K.S.; Sousa, C.S.; Viana, E.K.A.; Souza, H.C.A.; Souza, M.D.A.; Ribeiro, A.S.N.; Vale, V.d.S.d.; Islam, M.T.; Araújo, J.L.; Rocha, J.A. Bioactive Components of *Myracrodruon urundeuva* against SARS-CoV-2: A Computational Study. *Drugs Drug Candidates* **2023**, *2*, 781–795. <https://doi.org/10.3390/ddc2040039>

Academic Editors: Jean Jacques Vanden Eynde and Annie Mayence

Received: 12 August 2023

Revised: 21 September 2023

Accepted: 21 September 2023

Published: 27 September 2023



Copyright: © 2023 by the authors. Licensee MDPI, Basel, Switzerland. This article is an open access article distributed under the terms and conditions of the Creative Commons Attribution (CC BY) license (<https://creativecommons.org/licenses/by/4.0/>).

1. Introduction

The severe acute respiratory distress syndrome coronavirus 2 (SARS-CoV-2) is what causes the pandemic novel coronavirus disease 2019 (COVID-19). It was first identified in December 2019 in the city of Wuhan, China. The main clinical symptoms of COVID-19 include dry cough, dyspnea, fever, and bilateral pulmonary infiltrates [1]. Since the beginning of its journey, this virus has generated great challenges for all nations worldwide, and for this reason, it has been identified as one of the major global burdens. SARS-CoV-2 belongs to the family *Coronaviridae*. It is a single-stranded RNA virus. It has a positive reading sense, a nucleocapsid, and spike proteins [2]. This newest strain is highly contagious and potentially fatal, leading to the deaths of a total of 6,125,929 people and 481,521,638 confirmed cases worldwide as of 28 March 2022, according to the COVID-19 Panel of the Center for Systems Science and Engineering (CSSE) at Johns Hopkins University (JHU) (<https://coronavirus.jhu.edu/map.html>, accessed on 28 March 2022) [3].

SARS-CoV-2 transmits through direct contact through droplets and feces spread by an infected individual's cough, sneeze, or even talk and breathe less than one meter away

to susceptible persons [4]. Its incubation period corresponds to 5 or 6 days (which can be extended to 14 days). It can damage the alveoli, thereby resulting in acute pneumonia [5]. Injuries to the alveoli can also lead to some severe consequences, including respiratory distress, septic shock, multiple organ failure, and even the death of the patient through cardiorespiratory arrest [6]. Besides this, this viral infection is evidently causing liver disease and neurological problems [7]. However, the susceptibility and severity of COVID-19 depend on the type, age, and histopathological status of patients. For example, in Brazil, most of the COVID-19 cases were seen in patients with advanced ages. The medicinal scientists demonstrate that it is due to the reduced power of their immune functions [8].

Natural products are the basis of modern medicine. Over 25% of modern drugs are derived from nature. Therefore, bioactives from natural sources remain popular for study and research, especially in the pharmaceutical and biomedical fields. Research evidence suggests that natural compounds are capable of fighting against SARS-CoV-2 [9]. The plant *Myracrodruon urundeuva* F.F. and M.F. Aleme is commonly known as Aroeira do Serto in Brazil. It is used in traditional Northeastern medicine. It contains many important secondary metabolites, including tannins and chalcones, that are great sources for antioxidant, anti-inflammatory, and neuroprotective agents [10]. Several studies report that natural medicines can treat viral infections; for example, tea components can fight against flu, bronchitis [11], and gynecological infectious diseases [12]. Many studies demonstrate that this type of extract has potential antioxidant, anti-inflammatory, and healing properties [13]. Certain chemical groups, for example, flavonoids and phenolics, prevent oxidative stress that results from some diseases, including infections, atherosclerosis, diabetes, and neurodegenerative diseases [14].

The computational techniques used in bioinformatics are a gift for modern drug discovery and development. These reduce time and costs, thus accelerating *in vitro* and *in vivo* studies by facilitating the organization of data and assisting in the right choice of targets or hypotheses to be tested on the bench [15]. These tools are helpful for the design and development of new drugs, vaccines, and alternative therapeutics. One of these techniques is computer simulation through molecular docking studies, which is widely used in modern drug design. It is due to molecular docking's ability to predict with a substantial degree of precision the conformations and orientation of a small molecule (a ligand) within the binding sites of a macromolecular target (a protein), called a receptor [16]. Thus, in its most primitive form, it reproduces the concept of "key-lock" proposed by Emil Fischer in 1894, where the "key" (substrate) fits properly into the cavity (active site) of the "lock" (enzyme or receptor) for the productive biochemical reaction to occur [17]. The results obtained in these computational assays are given in terms of the free binding energy (kcal.mol^{-1}) necessary for the ligand-protein interaction to occur easily; in this way, the molecule that presents the lowest amount of energy needed to bind to the active site will be the one that, theoretically, will present the best result before the biological activity [18].

Understanding the overall facts, we aimed to identify new promising molecules from *M. urundeuva* against SARS-CoV-2 through molecular docking studies, where all possible active constituents of the plant were screened against four functional proteins of the virus, namely, Spike, M^{Pro}, ACE2, and RBD.

2. Results and Discussion

After selecting 44 chemical constituents of *M. urundeuva* [19–23], 176 dockings were performed (Table S1), of which 3 stood out by obtaining a lower binding energy, less than $-9.2 \text{ kcal.mol}^{-1}$. However, by expanding this range to values below $-8.5 \text{ kcal.mol}^{-1}$, a greater number of results were obtained (Table 1; Figure 1A,B) that were considered satisfactory and corresponded to 8.56% (groups 10, 11, and 12, Figure 2).

Table 1. Molecular reference parameters, referring to groups 10, 11, and 12, between the selected chemical constituents of *Myracrodruon urundeuva* and the target proteins of SARS-CoV-2.

Complex (Ligand–Protein)	ΔG_{bind}^a (kcal.mol ⁻¹)	Amino Acids That Interact by Hydrogen Bonding	Amino Acids That Interact by Hydrophobic Bonding
Agathisflavone/Spike	−9.7	His519, His49, Ser967, Asp571	Val42, Asp40, Asp568, Agr567, Agr44, Lys964, Leu518
Agathisflavone/RBD	−9.7	Lys417, Asn33, Asp30, Phe390, Ser494, Asp405	Ala387, Pre389, Leu455, Tyr495, Agr403, Asp38, Tyr453, His34, Glu37, Arg393, Tyr505, Ala386
Agathisflavone/M ^{Pro}	−9.3	Glu166, Phe140	Thr190, Gln189, His41, Met49, Met165, His164, Cys145, Leu141
Quercetin/Spike	−9.0	Arg100, Leu977, Thr573, Phe855, Tyr741	Gly744, Leu966, Val976, Thr547, Leu546, Asn978, Thr572, Met740, Asn856
Gallocatechin gallate /M ^{Pro}	−9.0	Phe140, Thr26, Ser144, His163, Leu141, Glu166	His172, Asn142, Leu27, Gly143, Thr25, Cys145, Met49, His41, Arg188, Asp187, Gln189, Met165
Taxifolin/Spike	−9.0	Ile742, Tyr741, Asn978	Ile587, Thr573, Val976, Leu977, Gly744, Arg1000, Leu966, Thr572, Gly744, Asn856, Gly548, Asn978, Thr547, Leu546, Val976, Thr527, Leu966
Luteolin/Spike	−9.0	Met740, Phe855, Thr573, Arg1000, Tyr741	Arg188, Met49, His164, Met165, Gly143, Cys145, Gln168, His41
Quercitrin/M ^{Pro}	−9.0	Asp187, Asn142, Leu141, Ser144, His163, Glu166, Tyr54	Ile587, Asn978, Val976, Leu977, Gly744, Arg1000, Thr572, Thr573
Eriodictiol/Spike	−8.9	Asn856, Ile742, Tyr741	Asn856, Gly744, Asn978, Leu546, Thr547, Val976, Thr572, Leu966
Apigenin/Spike	−8.7	Phe855, Thr573, Arg1000, Tyr741, Met740,	Asp568, Ile569, Arg567, Gly757, Asn969, Leu754, Gln755
Gallocatechin gallate/Spike	−8.7	His49, Arg44, Asp40, Asp571, Ser968, Ser967,	His519, Arg567, Thr430, Leu518, Glu516, Asp571, Asn969,
Naringenin/Spike	−8.7	Val976, Ser974, Arg983, Ile973, Asp979, Ser975	Val976, Pro589, Thr573, Phe855, Thr572
Cryptochlorogenic acid/Spike	−8.6	Arg1000, Ser975, Leu977, Asn978, Asn856, Ala570, Leu966	Asn856, Thr572, Ile587, Phe589, Phe855, Gly548, Thr573
Feruloyl-D-quinic acid/Spike	−8.6	Arg1000, Ser975, Leu977, Asn978, Asp568, Thr549, Gly744	
Gallocatechin/Spike	−8.6	Phe855, Thr549, Thr573, Thr572, Leu977, Gly744, Arg1000, Tyr741, Met740,	Pre589, Ile587, Asn856, Phe541

Our molecular docking process evaluated different spatial conformations of the ligand, which enabled us to identify the potential bioactive compounds that are most likely able to couple at the active site of the target protein. For each result, the respective bond-free energies were obtained in order to consider the lowest possible value due to the spontaneity of the reaction ($\Delta G < 0$) [24].

The spike protein (6VXX) helps SARS-CoV-2 enter human cells [25]. Thus, it is one of the main therapeutic targets to prevent the entry of viruses into humans (Figure 3). Among the chemical compounds of the tested herb, agathisflavone is evidently promising for its anti-inflammatory, antibacterial, and healing properties [26]. Our study also demonstrated that agathisflavone showed potential interaction capacity with the 6VXX.

The complex formed with agathisflavone obtained a free bond energy equal to -9.7 kcal.mol⁻¹ (Figure 4). It interacted directly with four amino acids by hydrogen bond (His519, His49, Ser967, and Asp571) and seven amino acids by hydrophobic bond (Val42, Asp40, Asp568, Agr567, Agr44, Lys964, and Leu518). Casalino et al. [27] stated that, by blocking the spike protein or modulating its conformational state through chemical interactions, it is possible to interfere directly with its binding capacity with the ACE2 receptor (the receptor that is responsible for the entrance of SARS-CoV-2 in humans). Thus,

the negative value indicates greater spontaneity, stability, and, consequently, the efficacy of the ligand in inhibiting its receptor [28].

The spike protein has two subunits, namely: S1, which is composed of the receptor binding domain (RBD) and is responsible for the direct association of this macromolecule with receptors present on the surface of host cells (ACE2), and S2, which is capable of causing membrane fusion [29]. Our findings demonstrate that agathisflavone interacted with the RBD (Figure 5) effectively, where the free bond energy corresponded to $-9.7 \text{ kcal.mol}^{-1}$. It resulted in intermolecular interactions through six bonds by hydrogen intrusion with the amino acid residues Lys417, Asn33, Asp30, Phe390, Ser494, and Asp405, and twelve bonds through hydrophobic intrusion with the amino acid residues Ala387, Pre389, Leu455, Tyr495, Agr403, Asp38, Tyr453, His34, Glu37, Arg393, Tyr505, and Ala386.

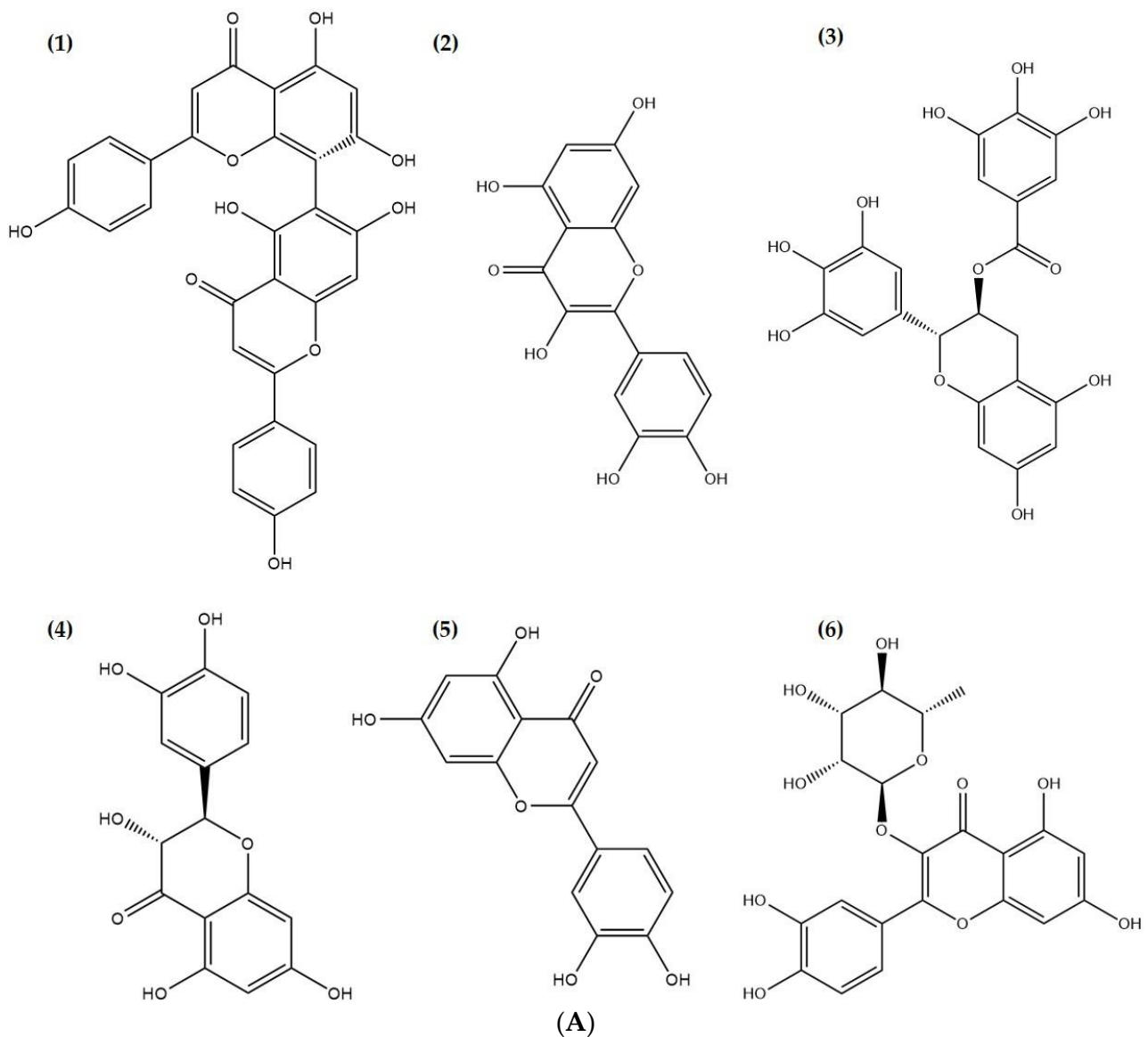


Figure 1. Cont.

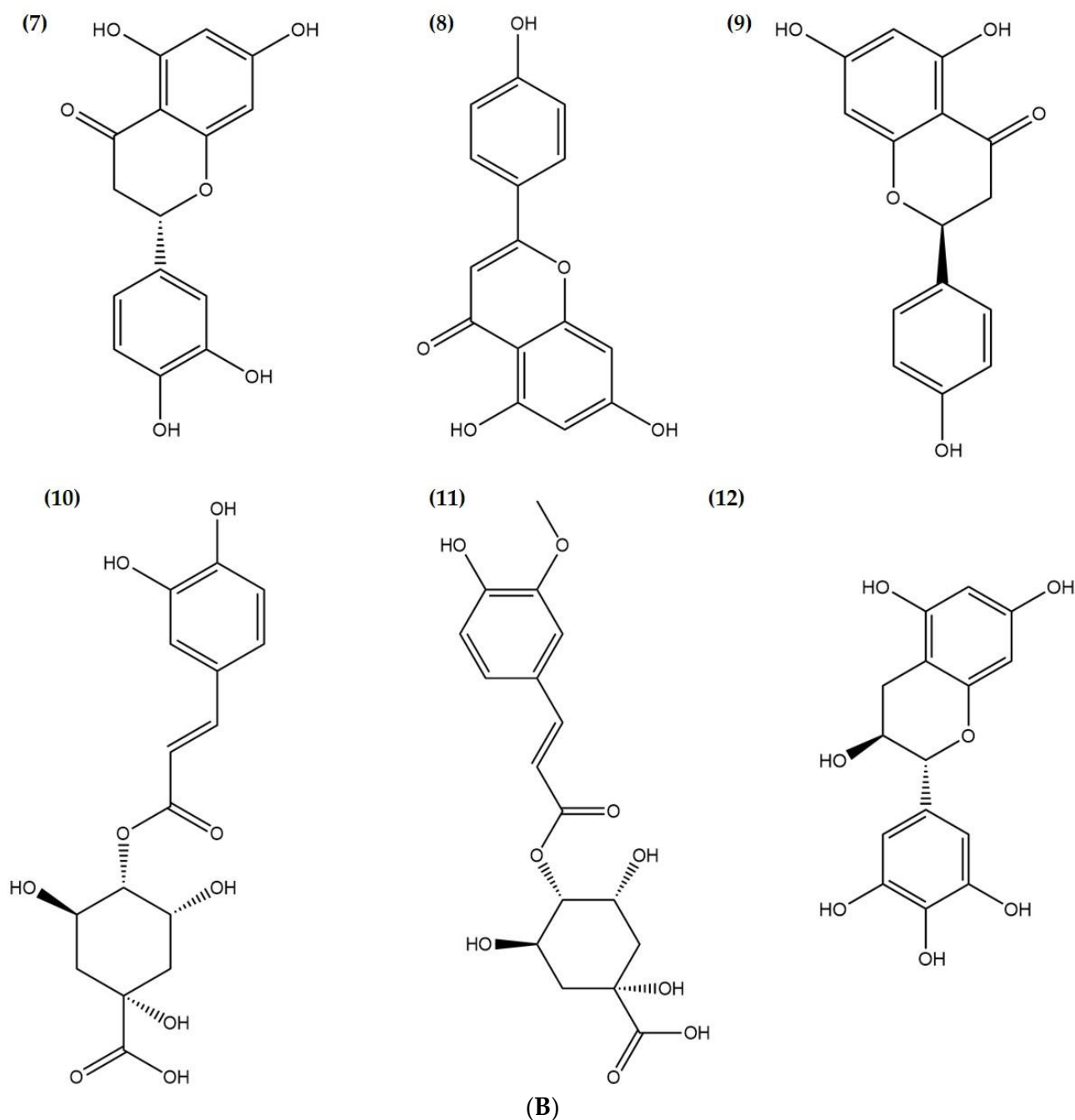


Figure 1. (A) Two-dimensional chemical structure of the chemical constituents of *Myracrodruon urundeuva* presenting the best results (groups 9, 10, and 11) through the molecular docking process (1 (Agathisflavone); 2 (Quercetin); 3 (Gallocatechin gallate); 4 (Taxifolin); 5 (Luteolin); 6 (Quercitrin)). (B) Two-dimensional chemical structure of the chemical constituents of *Myracrodruon urundeuva* presenting the best results (groups 9, 10, and 11) through the molecular docking process (7 (Eriodictiol); 8 (Apigenin); 9 (Naringenin); 10 (Cryptochlorogenic acid); 11 (Feruloyl-D-quinic acid) and 12 (Gallocatechin)).

The SARS-CoV-2 replicase gene makes the overlapping polyproteins pp1a and pp1ab. The main protease 3CL ($M^{P^{ro}}$) cuts them at 11 different places to make shorter nonstructural proteins that are important for its replication process [30]. If new molecules were added to or bound to this protease, the structure would change, which would have a direct effect on the copying process of viral RNA [31]. In this study, agathisflavone resulted in a free binding energy equal to $-9.3 \text{ kcal.mol}^{-1}$ (Figure 6) with two amino acids by hydrogen

bonding with the amino acid residues Glu166 and Phe140, while eight hydrophobic bonds were formed with the amino acid residues, namely, Thr190, Gln189, His41, Met49, Met165, His164, Cys145, and Leu141 of M^{Pro} of the virus.

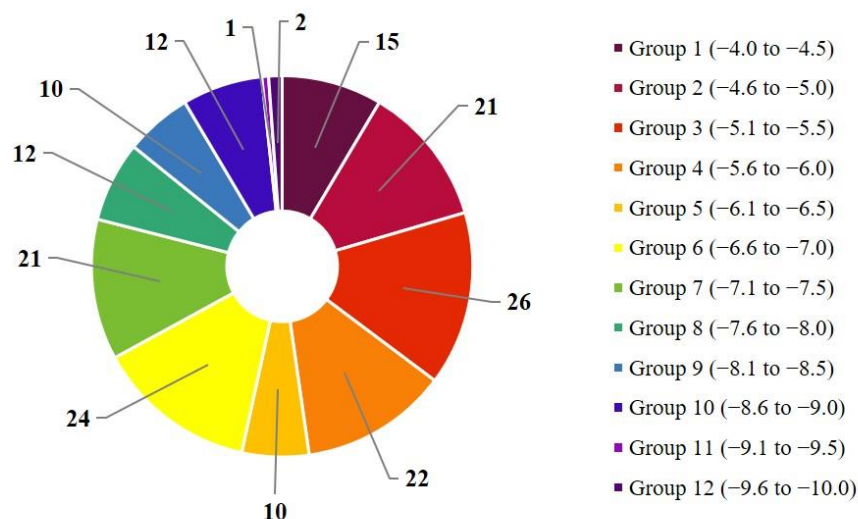


Figure 2. Total number of results, given in terms of binding free energy (kcal.mol⁻¹), sorted by categories.

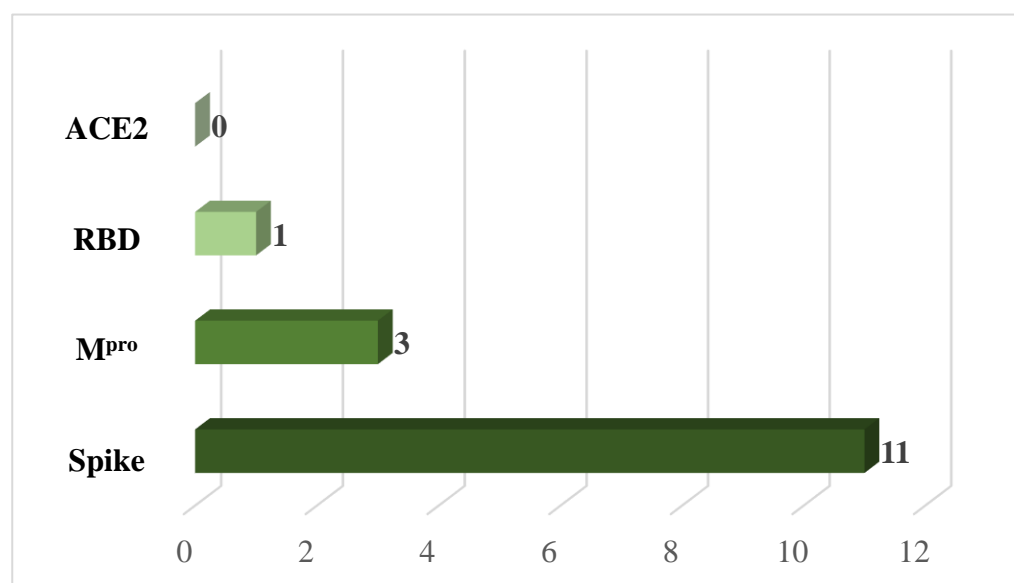


Figure 3. Proteins that stood out the most among the best results (groups 10, 11, and 12).

It is important to highlight that, in proteins, hydrogen bonds play a vital role in stabilizing their three-dimensional structure, influencing the way they unfold and interact with other molecules, being crucial for their stability. Hydrophobic interactions, on the other hand, mainly result in increased entropy of water molecules and new hydrogen bonds that arise when water molecules involving hydrophobic molecules come into contact with others, thus having specific entropic and enthalpic components. Even if the complexation of the hydrophobic ligand within the protein results in costs associated with the partial loss of translational, rotational, and conformational entropies of the ligand, the entropic gain of the solvent molecules displaced from the site is greater than these [32].

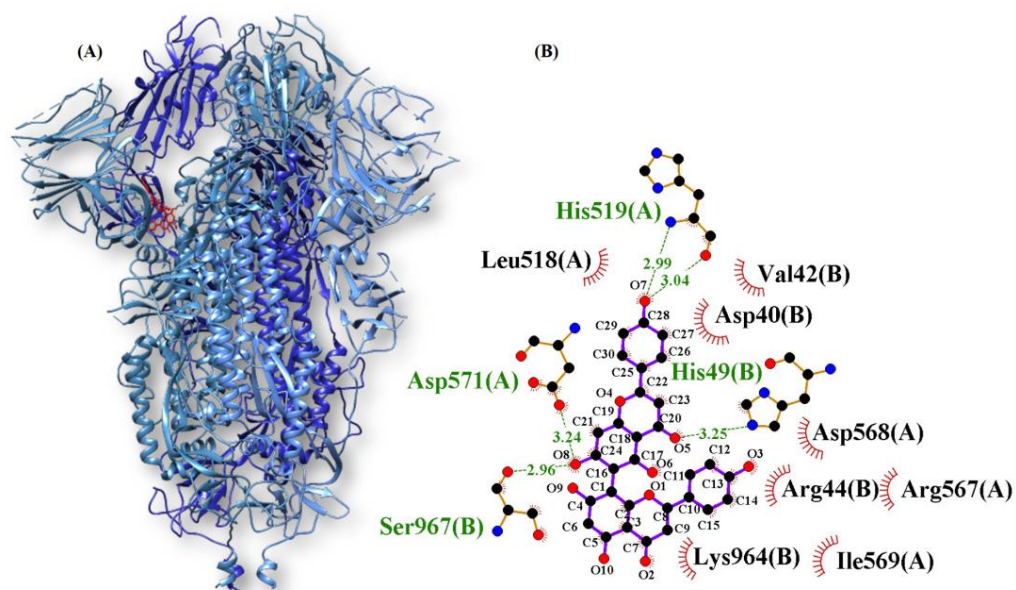


Figure 4. Agathisflavone interactions with the viral spike protein ((A) Three-dimensional structure between protein (blue) and ligand (red) and (B) LigPlot+ diagram of the interaction: hydrogen bonds (green) and hydrophobic bonds (red)).

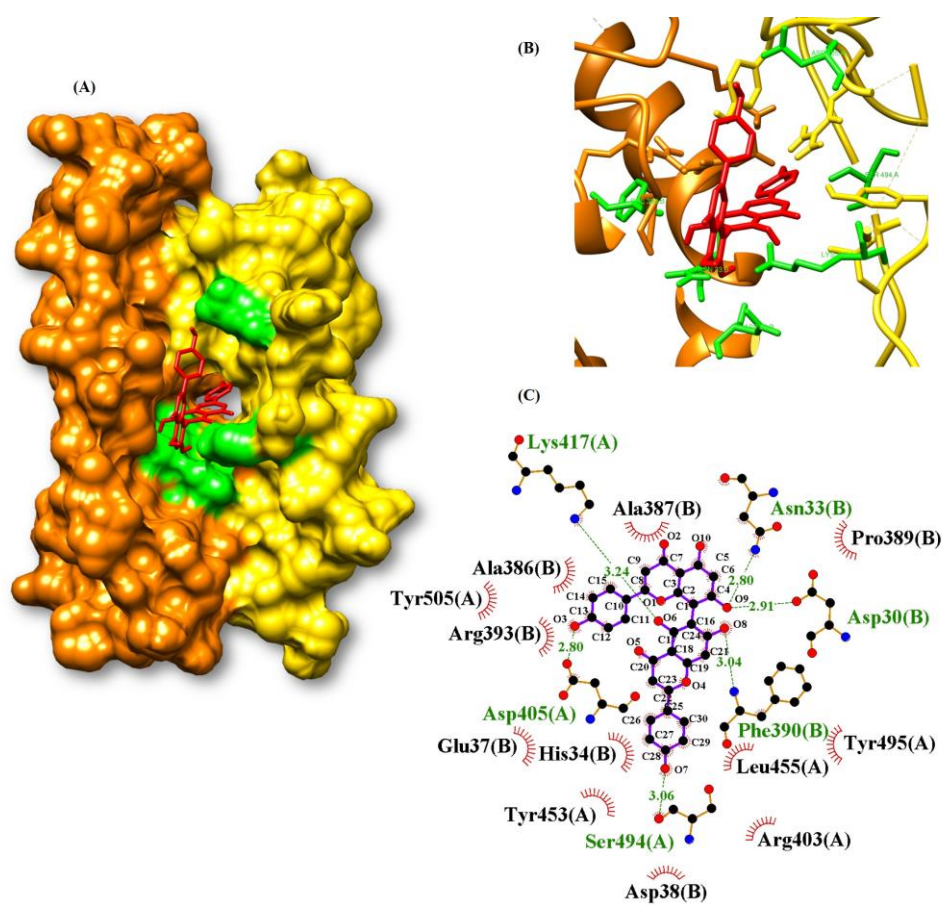


Figure 5. Agathisflavone interactions with the spike (orange)/ACE2 (yellow) (RBD) interaction site ((A) Three-dimensional structure between the protein and ligand (red), (B) Expansion of the docking region, and (C) LigPlot+ diagram of the interaction: hydrogen bonds (green) and hydrophobic bonds (red)).

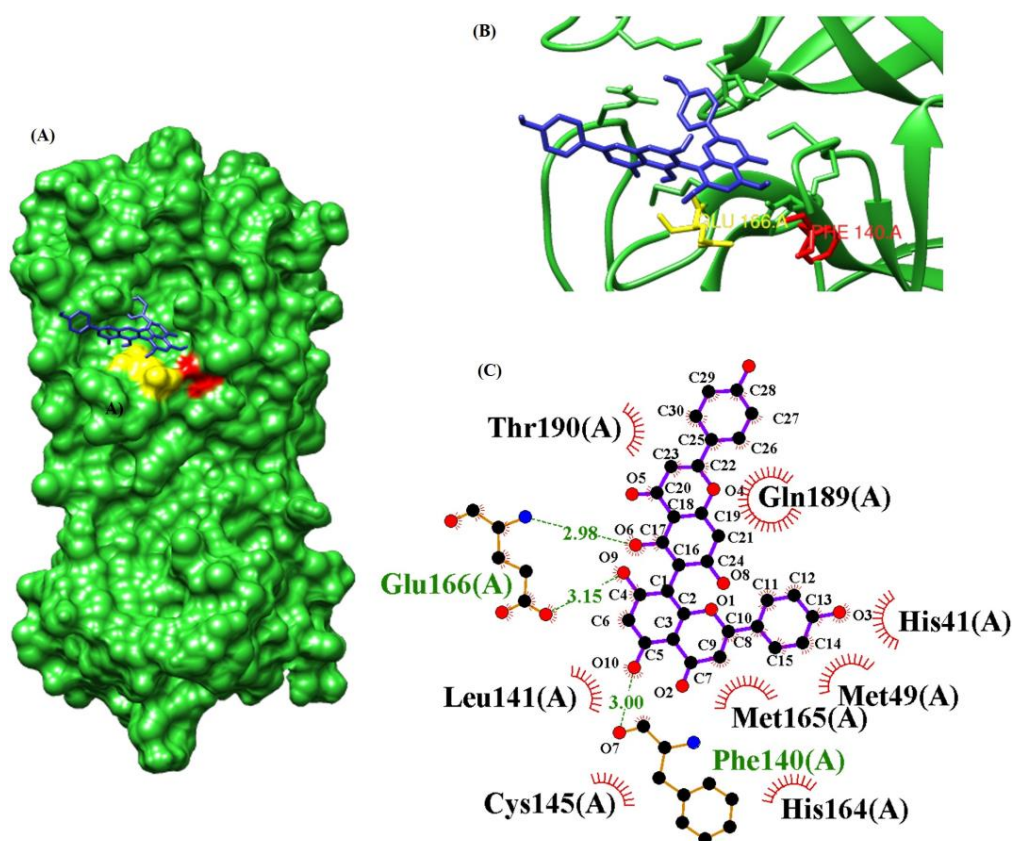


Figure 6. Agathisflavone interactions with the viral M^{Pro} protein ((A) Three-dimensional structure between protein (green) and ligand (blue), (B) Expansion of the docking region, and (C) LigPlot+ diagram of the interaction: hydrogen bonds (green) and hydrophobic bonds (red)).

The discovery of new therapeutic strategies to combat SARS-CoV-2 will also be one of the major approaches to the reuse of existing antiviral drugs against this virus. These strategies will also be capable of validating new and existing antiviral drugs against this deadly virus. For example, the international initiative Solidarity, led by the World Health Organization (WHO), began to recommend, in 2021, the emergency use of the drugs baricitinib, molnupiravir, and remdesivir [33,34] against SARS-CoV-2, which reduced the time and cost of new research since safety tests (preclinical and clinical), formulation protocols, and large-scale production have already been established. However, when these drugs were submitted to the molecular docking process to check their potential against SARS-CoV-2, none of them presented satisfactory results. Table 2 shows that all these drugs showed binding capacity with the targeted proteins less than or equal to $-8.6 \text{ kcal mol}^{-1}$. Interestingly, the chemical constituents of *M. urundeuva* belonging to groups 10, 11, and 12 showed better affinities than the abovementioned established drugs.

Table 2. Molecular affinity parameters referring to the drugs baricitinib, molnupiravir, and remdesivir with the target proteins of SARS-CoV-2.

Compounds	$\Delta G_{\text{bind}}^a \text{ (kcal.mol}^{-1}\text{)}$			
	ACE2 Protein	M ^{Pro} Protein	RBD Protein	Spike Protein
Baricitinib	-6.8	-7.9	-7.8	-8.0
Molnupiravir	-7.2	-6.7	-6.8	-7.9
Remdesivir	-7.3	-7.9	-7.6	-7.5

However, prior to starting clinical trials, it is crucial to understand the absorption, distribution, metabolism, excretion, and toxicity (ADMET) of a drug candidate [35]. A

survey conducted in 2001 by the Intercontinental Medical Statistics (IMS Health) suggests that 84% of the 50 most frequently used drugs in Europe and the United States are used via oral route [36]. This made medicinal scientists more interested in finding new bioactive principles that could be easily absorbed by the gastrointestinal tract [37]. Our in silico study demonstrates that the screened chemical compounds of the herb (groups 10, 11, and 12) showed high intestinal absorption potential in humans, ranging from 55.404 to 94.062% (except cryptochlorogenic acid and feruloyl-D-quinic acid) (Table 3).

Table 3. Absorption properties of the chemical constituents of *Myracrodruon urundeuva* belonging to groups 10, 11, and 12.

Compounds	Solubility in Water (log mol.L ⁻¹)	PCaco2 (Log Papp in 10 ⁻⁶ cm.s ⁻¹)	AIH%	P.Skin (log Kp)
Agathisflavone	-2.892	0.371	94.062	-2.735
Apigenin	-3.178	1.076	91.856	-2.736
Cryptochlorogenic acid	-2.854	-0.707	15.087	-2.735
Eriodictiol	-3.344	0.787	79.846	-2.736
Feruloyl-D-quinic acid	-2.776	-0.576	19.764	-2.735
Gallocatechin gallate	-2.895	-0.797	57.176	-2.735
Luteolin	-3.173	0.762	81.082	-2.735
Naringenin	-3.903	0.634	68.462	-2.735
Quercetin	-2.982	0.694	74.84	-2.735
Quercitrin	-3.132	-0.476	55.404	-2.735
Taxifolin	-3.031	-0.318	70.529	-2.735

Note: PCaco2: permeability of Caco-2 cells; AIH: intestinal absorption potential in humans; P.Skin: skin permeability.

The human colon adenocarcinoma (Caco-2) cells are frequently used to test the dissolution and permeation of water-soluble drugs and predict how well they will be absorbed after oral administration [38]. As suggested by the literature, chemical compounds with permeability coefficients lower than 1×10^{-6} cm/s, between 1 and 10×10^{-6} cm/s, and greater than 10×10^{-6} cm/s can be classified, respectively, as poorly absorbed (0–20%), moderately absorbed (20–70%), and well absorbed (70–100%), respectively [39,40]. The computational results aim to define the permeability based on this cell type by predicting the selected constituents' poor absorption. Regarding dermal permeability, log Kp values lower than -2.5 imply low absorption in the skin [41].

Another factor observed was the steady-state volume of distribution (VDss) (Table 4), a theoretical value referring to the total dose that a drug would need to be evenly distributed at the same concentration of blood plasma [38]. The VDss is considered low for log values less than -0.15 and high for values above -0.45 [42]. Therefore, the high VDss of the bioactives agathisflavone, cryptochlorogenic acid, and feruloyl-D-quinic acid indicate their better distribution in tissues than in plasma. Regarding the permeability of the blood–brain barrier (BBB), a structure that prevents and/or hinders the passage of substances from the blood to the central nervous system (CNS), none of the compounds can cross it since their BBB logs are <0.3 [39].

The Salmonella typhimurium mutation reversal assay, also called the Ames test, is widely used to check toxicological parameters, especially gene mutations caused by test substances [43]. Our in silico study suggested that eriodictiol, gallocatechin gallate, naringenin, quercetin, quercitrin, and taxifolin showed carcinogenicity, while others remained noncarcinogenic (Table 5).

On the other hand, the 50% lethal dose (LD₅₀) test predicts how much of a given substance is needed to kill 50% of a test population [44]. This parameter is necessary to check the therapeutic index and safety profile of bioactive substances. Our study suggests that feruloyl-D-quinic acid and naringenin were the most toxic and safe compounds, respectively. This is because the higher the lethal dose, the less dangerous the chemical is. In the same sense, our chronic oral toxicity in rats (LOAEL) suggests that agathisflavone, cryptochlorogenic acid, feruloyl-D-quinic acid, gallocatechin gallate, naringenin, quercetin,

and taxifolin can be ingested in greater quantities. Feruloyl-D-quinic acid might be used in a large dose to produce the desired effect without resulting in any potential side effects. The liver is the major metabolic site in our body. Thus, the safety of this organ is a foremost concern while developing and installing any drug candidate [45]. Our findings suggest that all the tested bioactive substances did not show hepatotoxicity. Additionally, these compounds did not show skin sensitization, suggesting their safety profiles in animals.

Table 4. Distribution properties of the chemical constituents of *Myracrodruon urundeuva* belonging to groups 10, 11, and 12.

Compounds	VD _{ss} (Human) (log L.Kg ⁻¹)	P.B.H (log BB)
Agathisflavone	−0.943	−2.192
Apigenin	−0.105	−0.951
Cryptochlorogenic acid	−1.495	−1.737
Eriodictiol	0.229	−1.180
Feruloyl-D-quinic acid	−1.738	−1.593
Gallocatechin gallate	0.050	−2.209
Luteolin	0.071	−1.199
Naringenin	−0.431	−1.449
Quercetin	0.310	−1.377
Quercitrin	−0.315	−2.027
Taxifolin	0.547	−1.328

Note: VD_{ss}: Apparent volume of distribution at steady state; P.B.H: permeability of the blood–brain barrier.

Table 5. Toxicological properties of the chemical constituents of *Myracrodruon urundeuva* plant belonging to groups 10, 11, and 12.

Compounds	T.AMES	D.M.T (log mg.kg ⁻¹ .day ⁻¹)	T.A.O (LD ₅₀) (mol.kg ⁻¹)	T.C.O (LOAEL) (log mg.kg ⁻¹ .day ⁻¹)	S.Skin	Hep
Agathisflavone	No	0.425	2.467	3.285	No	No
Apigenin	No	0.931	2.376	1.461	No	No
Cryptochlorogenic acid	No	1.379	2.219	3.503	No	No
Eriodictiol	Yes	0.395	2.229	1.893	No	No
Feruloyl-D-quinic acid	No	1.428	2.133	3.587	No	No
Gallocatechin gallate	Yes	0.481	2.654	4.085	No	No
Luteolin	No	0.975	2.450	1.833	No	No
Naringenin	Yes	0.989	3.573	3.556	No	No
Quercetin	Yes	0.954	2.308	3.134	No	No
Quercitrin	Yes	0.878	2.930	2.826	No	No
Taxifolin	Yes	0.886	2.245	3.256	No	No

Note: T.AMES: AMES toxicity; D.M.T: maximum tolerated dose in humans; T.A.O: acute oral toxicity in rats; T.C.O: chronic oral toxicity in rats; S.Skin: skin sensitization; Hep.: Hepatotoxicity.

Prior to the discovery of this new strain (SARS-CoV-2), the genomes of six species of coronavirus (CoVs) had already been fully sequenced and reported to GenBank (in November 2002). Four of these species, including HCoV-229E, HCoV-NL63, HCoV-OC43, and HCoV-HKU1, cause only relatively mild autoimmune infections with limiting respiratory symptoms. The others, SARS-CoV-1 and MERS-CoV, are highly pathogenic and capable of provoking severe acute respiratory syndrome with high mortality rates [46].

Its variants are classified according to the lineage and mutation of its components. As a result, viruses belonging to the same lineage but containing different subsets of mutations can be classified as different variants. The variants are characterized by their transmissibility, disease severity, and ability to escape humoral immunity [47].

Currently, the omicron EG.5 variant is the latest to be labeled as a “variant of interest” by the World Health Organization (WHO), joining the current ranks of XBB.1.16 and XBB.1.5.

The new designation, made as part of an initial risk assessment, reflects its “notable increase” in global prevalence during the second half of 2023 (https://www.who.int/docs/default-source/coronaviruse/09082023eg.5_ire_final.pdf, accessed on 4 September 2023) [48]. The potential of variants to escape naturally induced immunity and vaccine-induced immunity makes it a priority to develop next-generation vaccines and drugs that trigger broadly neutralizing activity against current and potential future variants.

Thus, with the aid of computational biology to obtain experimental results in vitro, the analyses carried out during this research were able to identify a promising bioactive principle for the treatment of COVID-19, coming from a native plant of the Brazilian caatinga and cerrado; its inhibitory capacity of the proteins vital for the development of SARS-CoV-2 can produce positive reflexes for the patient and for society in terms of improvement and quality of life.

Nowadays, the world’s largest pharmaceutical industries have research programs in the area of natural products, as they offer several advantages, for example, the large number of chemical structures and saving time and resources. In this context, regarding *M. urundeuva*, for presenting great pharmacological use, its bark has anti-inflammatory, astringent, antiallergic, and healing properties, the roots are used in the treatment of rheumatism, and the leaves are indicated for the treatment of ulcers [49], this plant becomes a promising source of raw material.

3. Materials and Methods

3.1. Selection of Chemical Compounds of *Myracrodruon urundeuva*

Searches were made in national and international databases for selecting chemical compounds of *M. urundeuva*, namely: Scientific Electronic Library Online (SciELO), Capes journal portal, Regional Portal of the Virtual Health Library (Bireme), National Center for Biotechnology Information (PubMed), Thomson Reuters (Web of Science), Elsevier Group (Scopus), Science Direct, and Google Scholar. For this, we used published papers using the common keyword “*Myracrodruon urundeuva*”, which was then paired with “phytochemicals”, “chemical constituents”, or “phytochemistry”. After this, the selected chemical structures were acquired through the PubChem platform (<https://pubchem.ncbi.nlm.nih.gov/>, accessed on 10 August 2022) [50] for further molecular optimization.

3.2. Determination of the Active Site

The active sites of the SARS-CoV-2 proteins were determined using the GASS-WEB server, a tool that works with calculations using the method of genetic algorithms looking for corresponding residues stored in databases such as the Catalytic Site Atlas (CSA), National Center for Biotechnology Information (NCBI), and Protein Data Bank (PDB). The models undergo calculations of root-mean-square deviation (RMSD) comparing the model and the residues surveyed. This methodology was able to identify 90% of the catalytic active sites cataloged [51]. The methodology of searching for the active site by similarity can be observed by Izidoro, Melo-Minardi, and Pappa [52].

3.3. Molecular Docking Study

The 3D structures of four viral proteins were obtained from the Protein Data Bank (PDB) (<http://www.rcsb.org/>, accessed 16 September 2022) [53] with the respective codes 6VXX (protein S or spike), 1R42 (angiotensin-converting enzyme, ACE2), and 6LU7 (main protein M^{Pro}), while RBD (Spike/ACE2 interaction site) was designed by Barros et al. (2020) [54]. They were then prepared by removing all water molecules and other groups, such as ions, using the Chimera v. 13.1 software [55]. In addition, polar hydrogen atoms were added, Gasteiger partial charges were calculated, and nonpolar hydrogens were mixed in both parts (ligand and protein) using the Autodock Tools (ADT) program, version 1.5.6. Docking was later performed through the Vina AutoDock program [56]. With the LIGPLOT program, used to automatically generate 2D schematic representations of the protein–ligand complexes from the standard input of PDB files, we obtained illustrations

of the points of interactions by hydrogen bridges and hydrophobic bonds between the chemical constituents and amino acid residues of the viral proteins [57].

3.4. ADME-TOX Prediction

The prediction of pharmaceutical parameters was performed using the online tool pkCSM (pharmacokinetics) (<https://biosig.lab.uq.edu.au/pkcsm/>, accessed on 12 February 2023) [58]. Our in silico study also evaluated the ADMET profiles of the bioactives, which include absorption (Caco-2 permeability, water solubility, human intestinal absorption, P-glycoprotein substrate, P-glycoprotein I and II inhibitors, skin permeability), distribution (VDss), unbound fraction, BBB and CNS permeability, metabolism (cytochrome P450 inhibitors, CYP2D6/CYP3A4 substrate), excretion (renal OCT2 substrate, total drug clearance), and toxicity (Rat LD₅₀, Ames toxicity, *Tetrahymena pyriformis* toxicity, minnow toxicity, maximum tolerated dose, chronic oral toxicity in rats, hepatotoxicity, skin sensitization) [59].

4. Conclusions

SARS-CoV-2 has been evidently producing negative biomedical and epidemiological effects on a global scale, directly impacting all dimensions of life, such as social, economic, political, and cultural spheres. Current immunity obtained by vaccines is quite effective in COVID-19, despite its unavoidable health problems such as unequal access to immunizers and the emergence of new variants, which reinforce the need for the search for new and effective alternative treatment options. Knowing this fact, we performed this study using 44 phytochemicals from a hopeful medicinal herb called *M. urundeuva*. Our findings reveal that the agathisflavone of the plant showed good molecular affinity (-9.3 to -9.7 kcal.mol⁻¹) with the vital proteins (Spike, RDB, and M^{Pro}), suggesting its potentiality against this deadly pathogen. This molecule also exhibited better binding affinity than the reference antiviral drugs used in SARS-CoV-2. Further, pharmacokinetic profiling of agathisflavone also demonstrates that it has a high degree of solubility and low toxicity. It also did not show skin sensitization or carcinogenicity in our in silico ADMET study. However, our findings are based on computational evaluation; therefore, it would be highly appreciable to perform in vivo studies to verify the efficacy and elucidate their exact mechanisms against this virus.

Supplementary Materials: The following supporting information can be downloaded at: <https://www.mdpi.com/article/10.3390/ddc2040039/s1>, Table S1: Molecular affinity parameters performed by the vina method in ΔG_{bind} (kcal.mol⁻¹) between the chemical constituents of the *M. urundeuva* plant with the proteins ECA2, M^{Pro}, RBD and Spike of the novel coronavirus COVID-19. References [19–23] are cited in the supplementary materials.

Author Contributions: Conceptualization, S.K.S.A., C.S.S., E.K.A.V., H.C.A.S., M.D.A.S., A.S.N.R., V.d.S.d.V., M.T.I., J.L.A. and J.A.R.; data curation, J.A.R.; formal analysis, C.S.S.; investigation, S.K.S.A., C.S.S., E.K.A.V., H.C.A.S., M.D.A.S., A.S.N.R., V.d.S.d.V., J.L.A. and J.A.R.; methodology, S.K.S.A., C.S.S., E.K.A.V., H.C.A.S., M.D.A.S., A.S.N.R. and V.d.S.d.V.; supervision, J.L.A. and J.A.R.; validation, M.T.I.; writing—original draft, S.K.S.A., E.K.A.V., M.T.I., J.L.A. and J.A.R.; writing—review and editing, S.K.S.A., M.T.I., J.L.A. and J.A.R. All authors have read and agreed to the published version of the manuscript.

Funding: The authors are grateful to the Foundation for Scientific Technological Research and Development of Maranhão—FAPEMA (UNIVERSAL-06509/22) and to the State Government of Maranhão and the Secretariat of State for Science, Technology and Innovation—SECTI for their support with the study scholarship and the Federal University of Maranhão—UFMA for their incentive and this research was funded by the National Council for Scientific and Technological Development (CNPq).

Institutional Review Board Statement: Not applicable.

Informed Consent Statement: Not applicable.

Data Availability Statement: Not applicable.

Conflicts of Interest: The authors declare no conflict of interest.

References

1. Dourado, L.; Caetano, L.; Marques, M.; Penna, U.; Costa, C.; Arruda, F.; Libera, L. Estudo da história natural da COVID-19 e epidemiology of SARS-CoV-2 infection: A descriptive review of the literature. *Braz. J. Surg. Clin. Res.* **2020**, *33*, 46–56.
2. Oliveira, M.; Robinson, A.; Siqueira, M. Knowing SARS-CoV-2 and COVID-19. In *Health Diplomacy and COVID-19: Reflections Halfway*, 1st ed.; Fonseca, L., Ed.; Fiocruz: São Paulo, Brazil, 2020; pp. 69–82.
3. Johns Hopkins Coronavirus Resource Center. Available online: <https://coronavirus.jhu.edu/map.html> (accessed on 11 November 2022).
4. Nascimento, L.; Marchiori, M.; Field, V.; Zini, M. SARS-CoV-2 and COVID-19: Pathophysiological and immunological aspects, diagnostic strategies and vaccine development. *Rev. Interdiscip. Saúde Educ.* **2020**, *1*, 122–158. [[CrossRef](#)]
5. Schoeman, D.; Fielding, B. Coronavirus envelope protein: Current knowledge. *Viol. J.* **2019**, *16*, 69. [[CrossRef](#)]
6. Lin, L.; Lu, L.; Cao, W.; Li, T. Hypothesis for potential pathogenesis of SARS-CoV-2 infection—a review of immune changes in patients with viral pneumonia. *Emerg. Microbes Infect.* **2020**, *9*, 727–732. [[CrossRef](#)] [[PubMed](#)]
7. Marra, M.A.; Jones, S.J.M.; Astell, C.R.; Holt, R.A.; Brooks-Wilson, A.; Butterfield, Y.S.N.; Khattra, J.; Asano, J.K.; Barber, S.A.; Chan, S.Y.; et al. The Genome Sequence of the SARS-Associated Coronavirus. *Science* **2003**, *300*, 1399–1404. [[CrossRef](#)] [[PubMed](#)]
8. Barbosa, I.; Galvão, M.; Souza, T.; Gomes, S.; Medeiros, A.; Lima, K. Incidence of and mortality from COVID-19 in the older Brazilian population and its relationship with contextual indicators: An ecological study. *Rev. Bras. Geriatr. Gerontol.* **2020**, *23*, 2017. [[CrossRef](#)]
9. Antonio, A.; Wiedemann, L.; Junior, V. Natural products' role against COVID-19. *RSC Adv.* **2020**, *10*, 23379–23393. [[CrossRef](#)]
10. Domingos, F.; Silva, M. Use, knowledge and conservation of *Myracrodruon urundeuva*: A systematic review. *Res. Soc. Dev.* **2020**, *9*, 8851. [[CrossRef](#)]
11. Amaral, E.A.; Silva, R.M.G. Evaluation of the acute toxicity of angico (*Anadenanthera falcata*), pau-santo (*Kilmeyera coreacea*), aroeira (*Myracrodruon urundeuva*) and São João vine (*Pyrostegia venusta*), by means of the bioassay with *Artemia salina*. *J. Serv. Res.* **2008**, *5*, 1–16.
12. Maia, G. *Caatinga, Trees and Shrubs and Their Utilities*, 1st ed.; D & Z: São Paulo, Brazil, 2004.
13. Souza, S.; Aquino, L.; Milach, A.; Bandeira, M.; Nobre, M.; Viana, G. Antiinflammatory and antiulcer properties of tannins from *Myracrodruon urundeuva* Allemão (Anacardiaceae) in Rodents. *Phytother. Res.* **2007**, *21*, 2020–2225. [[CrossRef](#)]
14. Asadi, S.; Ahmadiani, A.; Esmaili, M.; Sonboli, A.; Ansari, N.; Khodagholi, F. In vitro antioxidant activities and an investigation of neuroprotection by six *Salvia* species from Iran: A comparative study. *FTC* **2010**, *48*, 1341–1349. [[CrossRef](#)] [[PubMed](#)]
15. Filho, F.; Nascimento, K.; Santos, W.; Frazão, N. Study of acetylcholinesterase inhibition by molecular docking: Application in the treatment of Alzheimer's disease. *Ed. S. Health.* **2020**, *7*, 1–18. [[CrossRef](#)]
16. Ferreira, L.; Santos, R.; Oliva, G.; Andricopulo, A. Molecular docking and structure-based drug design strategies. *Molecules* **2015**, *20*, 13384–13421. [[CrossRef](#)] [[PubMed](#)]
17. Tripathi, A.; Bankaitis, V. Molecular Docking: From Lock and Key to Combination Lock. *J. Mol. Med. Clin. Appl.* **2017**, *2*, 106. [[CrossRef](#)]
18. Dias, R.; Azevedo, J.; Walter, F. Molecular Docking Algorithms. *Curr. Drug Targets* **2008**, *9*, 1040–1047. [[CrossRef](#)] [[PubMed](#)]
19. Castro, C.B. *Chemical Profile and Cytotoxic Activity of Leaf, Branch and Bark Extracts of Aroeira-Do-Sertão (Myracrodruon urundeuva All.): Metabolomic and Chemometric Approach*; Monograph (Graduation in Chemistry); Federal University of Ceará: Fortaleza, Brazil, 2016.
20. Figueredo, F.; Lucena, B.; Tintino, S.; Matias, E.; Leite, N.; Andrade, J.; Nogueira, L.; Morais, E.; Costa, J.; Coutinho, H.; et al. Chemical composition and evaluation of modulatory of the antibiotic activity from extract and essential oil of *Myracrodruon urundeuva*. *Pharm. Biol.* **2014**, *52*, 560–565. [[CrossRef](#)]
21. Costa, O.B.; Mennezi, C.; Benedito, L.; Resck, I.; Viera, F.; Bizzo, H. Essential oil constituents and yields from leaves of *Blepharocalyx salicifolius* (Kunt) O. Berg and *Myracrodruon urundeuva* (Allemão) collected during daytime. *J. For. Res.* **2014**, *2014*, 982576. [[CrossRef](#)]
22. Alquino, N. Chemical Aspects of the Chemical-Pharmacological-Agronomic Study of Wild and Cultivated Aroeiras do Sertão (*Myracrodruon urundeuva* Fr. all). Ph.D. Thesis, Federal University of Ceará, Fortaleza, Brazil, 2017.
23. Pessoa, E.; Nicolette, R.; Araújo, T. The use of Anacardiaceae Family's vegetable extracts as natural skin-clearing agents: A review. *World J. Pharm. Res.* **2020**, *9*, 32–37. [[CrossRef](#)]
24. Ruyck, J.; Brysbaert, G.; Blossey, R.; Lensink, M. Molecular docking as a popular tool in drug design, an in silico travel. *Adv. Appl. Bioinform. Chem.* **2016**, *9*, 1–11. [[CrossRef](#)]
25. Smith, R.; Cavalcante, G. Potential therapeutic targets for COVID-19: An integrative review. *JCS HU-UFPI* **2021**, *4*, 18–25. [[CrossRef](#)]
26. Oliveira, Y.R.; Robinson, W.; Smith, P.; Pacheco, A.; Abreu, M. Anacardiaceae in the Traditional Medicine of Rural Communities of Piauí, Northeastern Brazil. *Ens. Ciências* **2022**, *26*, 32–42. [[CrossRef](#)]

27. Casalino, L.; Gaieb, Z.; Goldsmith, J.; Hjorth, C.; Dommer, A.; Harbison, A.; Fogarty, C.; Barros, E.; Taylor, B.; McLellan, J.; et al. Beyond Shielding: The Roles of Glycans in the SARS-CoV-2 Spike Protein. *ACS. Cent. Sci.* **2020**, *6*, 1722–1734. [[CrossRef](#)] [[PubMed](#)]
28. Junior, E.; Gonsalves, A. Molecular docking study of gsk-3 β enzyme inhibitors: A proposal for the treatment of bipolar disorder. *Rev. Ifes Sci.* **2019**, *5*, 243–256. [[CrossRef](#)]
29. Ord, M.; Faustova, I.; Loog, M. The sequence at Spike S1/S2 site enables cleavage by furin and phospho-regulation in SARS-CoV-2 but not in SARS-CoV-1 or MERS-CoV. *Sci. Rep.* **2020**, *10*, 16944. [[CrossRef](#)] [[PubMed](#)]
30. Qiao, J.; Li, Y.; Zeng, R.; Liu, F.; Luo, R.; Huang, C.; Wang, Y.; Zhang, J.; Quan, B.; Yang, S. SARS-CoV-2 Mpro inhibitors with antiviral activity in a transgenic mouse model. *Science* **2019**, *371*, 1374–1378. [[CrossRef](#)]
31. Kumar, S. COVID-19: A Drug Repurposing and Biomarker Identification by Using Comprehensive Gene-Disease Associations through Protein-Protein Interaction Network Analysis. *Preprints* **2020**, *1*, 2020030440. [[CrossRef](#)]
32. Bissantz, C.; Kuhn, B.; Stahl, M. A medicinal chemist's guide to molecular interactions. *J. Med. Chem.* **2010**, *22*, 5061–5084. [[CrossRef](#)]
33. Incerti, M.K.; Rosa, T.F.; Foletto, V.S.; Franco, L.N.; Hörner, R. Repurposing Medications for COVID-19: An Overview. *Health* **2022**, *48*, 1–5.
34. Robinson, M.; Facchainetti, V.; Aboud, K.; Penha, L.; Gomes, C. Repositioning of the drug baricitinib for the treatment of COVID-19. *Conjectures* **2022**, *22*, 306–321. [[CrossRef](#)]
35. Smith, D.; Padilha, I. In silico evaluation of pharmacokinetic properties of antileukemic compounds published by scientific journals. *Arch. Health. Sci.* **2022**, *30*, e04978. [[CrossRef](#)]
36. Lennernäs, H.; Abrahamsson, B. The use of biopharmaceutic classification of drugs in drug discovery and development: Current status and future extension. *J. Pharm. Pharmacol.* **2005**, *57*, 273–410. [[CrossRef](#)]
37. Jorgensen, W.; Duffy, E. Prediction of drug solubility from structure. *Adv. Drug Deliv. Rev.* **2002**, *54*, 355–366. [[CrossRef](#)]
38. Robinson, J.; Robinson, Z.; Storpirtis, S. In vitro models for determining drug absorption and predicting the dissolution/absorption ratio. *Rev. Bras. Cienc. Farm.* **2007**, *43*, 515–527. [[CrossRef](#)]
39. Fernandes, M.B.; Gonçalves, J.; Scotti, M.; Oliveira, A.; Tavares, L.; Storpirtis, S. Caco-2 cells cytotoxicity of nifuroxazide derivatives with potential activity against Methicillin-resistant *Staphylococcus aureus* (MRSA). *Toxicol. In Vitro.* **2012**, *26*, 535–540. [[CrossRef](#)] [[PubMed](#)]
40. Meanwell, N.A. Improving Drug Candidates by Design: A Focus on Physicochemical Properties as a Means of Improving Compound Disposition and Safety. *Chem. Res. Toxicol.* **2011**, *24*, 1420–1456. [[CrossRef](#)] [[PubMed](#)]
41. Pinheiro, R.; Júnior, A.; Zepeda, C.; Santos, L.; Pinto, L.; Cabral, O.; Soto, C. In silico analysis of the pharmacokinetic and toxicological profile of Zinc II thioglycolate complex [Zn(ATG)₂(OH)₂]. *Res. Soc. Dev.* **2022**, *11*, e44711629430. [[CrossRef](#)]
42. Holguín, N.M.; Frau, J.; Mitnik, D.G. Computational Pharmacokinetics Report, ADMET Study and Conceptual DFT-Based Estimation of the Chemical Reactivity Properties of Marine Cyclopeptides. *Chem. Open* **2021**, *10*, 1087–1157. [[CrossRef](#)]
43. Aiub, C.A.F.; Felzenszwalb, I. The principles of the Ames (*Salmonella*/microsome) test and its applicability. *Genet. Sch.* **2011**, *6*, 11–16. [[CrossRef](#)]
44. Pimentel, L.C.F.; Keys, C.; Robinson, L.; Alfonso, J. The unbelievable use of dangerous chemicals in the past. *Whoops. New.* **2006**, *29*, 1138–1149. [[CrossRef](#)]
45. Bertolami, M.C. Mechanisms of hepatotoxicity. *Arq. Bras. Cardiol.* **2005**, *85*, 25–27. [[CrossRef](#)]
46. Li, Y.; Chi, W.; Su, J.; Ferrall, L.; Hung, C.; Wu, T. Coronavirus vaccine development: From SARS and MERS to COVID-19. *J. Biomed. Sci.* **2020**, *27*, 104. [[CrossRef](#)]
47. Tao, K.; Tzou, F.L.; Nouhin, J.; Gupta, R.K.; Oliveira, T.; Kosakovsky, L.S.L.; Fera, D.; Shafer, R.W. The biological and clinical significance of emerging SARS-CoV-2 variants. *Nat. Rev. Genet.* **2021**, *22*, 757–773. [[CrossRef](#)]
48. World Health Organization. Available online: https://www.who.int/docs/default-source/coronaviruse/09082023eg.5_ire_final.pdf (accessed on 4 September 2023).
49. Robinson, R.; Fagundes, M.; Roberts, H.; Veloso, M. Ecological aspects of aroeira (*Myracrodruon urundeuva* Allemão- Anacardiaceae): Phenology and seed germination. *Rev. Árvore* **2008**, *32*, 233–243. [[CrossRef](#)]
50. PubChem. Available online: <https://pubchem.ncbi.nlm.nih.gov/> (accessed on 10 August 2022).
51. Morais, J.P.A.; Pappa, G.L.; Pires, D.E.V.; Izidoro, S.C. GASS-WEB: A web server for identifying enzyme active sites based on genetic algorithms. *Nucleic Acids Res.* **2017**, *45*, 315–319. [[CrossRef](#)]
52. Moraes, J.P.A.; Izidoro, S.C.; Melo-Minardi, R.C.; Pappa, G.L. GASS: Identifying enzyme active sites with genetic algorithms. *Bioinformatics* **2015**, *31*, 864–870. [[CrossRef](#)]
53. RCSB Protein Data Bank. Available online: <http://www.rcsb.org/> (accessed on 16 September 2022).
54. Barros, R.O.; Junior, F.; Perreira, W.; Oliveira, N.; Ramos, R. Interaction of Drug Candidates with Various SARS-CoV-2 Receptors: An in-Silico Study to Combat COVID-19. *J. Proteome Res.* **2020**, *19*, 4567–4575. [[CrossRef](#)]
55. Pettersen, E.F.; Goldbard, T.; Huang, C.; Couch, G.; Greenblatt, D.; Meng, L.; Ferrin, T. UCSF Chimera—A visualization system for exploratory research and analysis. *J. Comput. Chem.* **2004**, *25*, 1605–1612. [[CrossRef](#)] [[PubMed](#)]
56. Trott, O.; Olson, A.J. AutoDock Vina: Improving the speed and accuracy of docking with a new scoring function, efficient optimization, and multithreading. *J. Comput. Chem.* **2009**, *31*, 455–461. [[CrossRef](#)] [[PubMed](#)]

57. Wallace, A.C.; Laskowski, R.A.; Thornton, J.M. LIGPLOT: A program to generate schematic diagrams of protein-ligand interactions. *Protein Eng. Des. Sel.* **1995**, *8*, 127–134. [[CrossRef](#)] [[PubMed](#)]
58. pkCSM: Predicting Small-Molecule Pharmacokinetic Properties Using Graph-Based Signatures. Available online: <https://biosig.lab.uq.edu.au/pkcsm/> (accessed on 12 February 2023).
59. Rocha, J.A.; Rego, N.; Carvalho, B.; Silva, F.; Sousa, J.; Ramos, R.; Passos, I.; Maraes, J.; Lima, F. Computational quantum chemistry, molecular docking, and ADMET predictions of imidazole alkaloids of *Pilocarpus microphyllus* with schistosomicidal properties. *PLoS ONE* **2018**, *13*, e0198476. [[CrossRef](#)] [[PubMed](#)]

Disclaimer/Publisher's Note: The statements, opinions and data contained in all publications are solely those of the individual author(s) and contributor(s) and not of MDPI and/or the editor(s). MDPI and/or the editor(s) disclaim responsibility for any injury to people or property resulting from any ideas, methods, instructions or products referred to in the content.